

OBTAINING PRECISE CRITICAL DRAW RATIO OF DRAW RESONANCE IN MELT SPINNING BY NUMERICAL SIMULATION OF DIFFERENCE EQUATIONS

Ji-nan Cao*

*Industrial Research Institute Swinburne, Swinburne University of Technology, P.O. Box 218 Hawthorn,
Victoria 3122, Australia*

Abstract Direct difference methods have been used to solve the simultaneous non-linear partial differential equations for melt spinning without recourse to linearisation or perturbation approximation. The stability of each difference schemes was studied by error analysis using the Taylor series, and by comparison of the results obtained from numerical simulation with the logical value in melt spinning. It is found that computation with 19 digit long double precision has significantly simplified the stability problem of difference equations. Using this method, the precise critical draw ratio of draw resonance in an isothermal and uniform tension spinning of Newtonian fluids can be obtained in between 20.218 and 21.219, a figure consistent with 20.218 which was obtained by a linear perturbation approximation method by Kase and Denn. It thus has paved the way to computation of full information for unsteady melt spinning processes using the difference method.

Keywords: Draw resonance; Melt spinning; Newtonian fluid; Numerical simulation.

INTRODUCTION

To elucidate the mechanisms of macro molecular structure formation of polymers during processing, mathematical modelling has become an important tool in polymer engineering. The governing equations of polymer processes such as melt spinning and film casting in unsteady states, however, consist of simultaneous non-linear partial differential equations, which are not analytically soluble except in a few simplified cases. Numerical methods have to be employed and their results have played a meaningful role in interpreting the behaviour of a polymer fluid under processing^[1–9].

A linearised perturbation approximation for the governing equations has been employed to obtain the critical draw ratio of draw resonance of polymer fluids in melt spinning^[10–14]. An orthogonal collocation method was also found useful in obtaining the critical draw ratio of draw resonance^[15]. Ver dan Hout recently reduced the linearised stability problem to a single Volterra integral equation to investigate the critical draw ratio for draw resonance^[16]. These methods are valid and helpful, but do not provide full information such as spinline profiles and the exact wave form of the diameter of taken-up filament as a direct difference method does^[17–19]. Due to this distinct characteristic, direct difference methods deserve more attention than other numerical methods. Indeed they have been employed in the articles studying the relationship between kinematic waves and draw resonance as well^[20–22].

However, the stability issue remains a subject of research. In this paper, the numerical stability of three difference methods applicable to solving the simultaneous partial differential equations has been studied. The precise critical draw ratio for Newtonian polymer fluids was then calculated using the most stable method.

* Corresponding author: Ji-nan Cao, E-mail: Jcao@swin.edu.au

Received April 14, 2004; Revised May 28, 2004; Accepted May 31, 2005

NON-DIMENSIONAL GOVERNING EQUATIONS, BOUNDARY AND INITIAL CONDITIONS

The governing equations of melt spinning consist of a constitution equation and a continuity equation^[17],

$$\frac{\partial v}{\partial x} = \frac{F}{A\beta} \quad (1)$$

$$\frac{\partial A}{\partial t} + \frac{\partial(Av)}{\partial x} = 0 \quad (2)$$

where, A and v denote the cross-sectional area and velocity of a filament section at time, t , and distance, x , from the spinneret. F represents the spinning tension, and is a constant along the spinline but varies with time by definition of a uniform tension spinning. The symbol β is for elongational viscosity, which is a constant for Newtonian fluids ($\beta = \beta_0$).

The governing equations can be expressed in terms of non-dimensional variables:

$$\frac{\partial \psi}{\partial \zeta} = \frac{\xi}{\lambda} \quad (3)$$

$$\frac{\partial \lambda}{\partial \tau} + \frac{\partial(\lambda\psi)}{\partial \zeta} = 0. \quad (4a)$$

The continuity equation can be written in another form, which is entirely equivalent to Eq. (4a) for an analytical solution.

$$\frac{\partial \lambda}{\partial \tau} + \psi \frac{\partial \lambda}{\partial \zeta} + \xi = 0. \quad (4b)$$

The non-dimensional parameters are defined as follows:

$$\zeta = x/L \quad \text{distance from spinneret;}$$

$$\tau = tV_0/L \quad \text{time;}$$

$$\lambda(\zeta, \tau) = A/A_0 \quad \text{cross-sectional area;}$$

$$\psi(\zeta, \tau) = v/V_0 \quad \text{velocity of a filament;}$$

$$\xi(\zeta, \tau) = [F/(A_0 \beta_0)]L/V_0 \quad \text{spinning tension}$$

where, L , A_0 and V_0 are the length of a spinline, *i.e.* the distance from the spinneret to the take-up bobbin, the cross-sectional area at the spinneret and the extrusion rate, respectively.

The non-dimensional spinning tension, ξ , denotes a material parameter of polymer fluids. Being a function of temperature and shear rate, it is largely determined by, in particular, the molecular structure formation of the polymer fluid under processing. Therefore, computation of ξ from experimentally measured parameter, $\lambda(\zeta, \tau)$, is a mathematical approach to elucidate the mechanism of structure formation of a polymer in the process. In this study, however, only Newtonian fluids are addressed. Simultaneous Eqs. (3) and (4a) or Eqs. (3) and (4b) constitute of the governing equations of polymer fluids in melt spinning.

The non-dimensional boundary condition can be written as,

$$\psi(0, \tau) = 1.0. \quad (5)$$

Initial conditions vary according to what a simulation is aiming at. In this study, the initial conditions are so assumed that the take-up velocity has a small step increment, 0.1%, at non-dimensional time 0; the new take-up velocity is then kept constant. By assuming this, we aim to understand how the cross-sectional area of a polymer fluid of the taken-up filament $\lambda(1, \tau)$ responds to the perturbation in take-up velocity, $\psi(1, \tau)$. The mathematical expression for the above statement is written,

$$\psi(1, \tau) = \begin{cases} \psi_w & \text{when } \tau < 0 \\ 1.001\psi_w & \text{when } \tau \geq 0 \end{cases} \quad (6)$$

where, ψ_w is a constant greater than unit, expressing the draw ratio of a spinning process.

FINITE DIFFERENCE METHODS AND COMPUTATIONAL PROCEDURES

There are three different difference schemes applicable to solving the differential equations.

Method A:

$$\psi_{i+1,j} = \psi_{i,j} + \xi_{i,j} \frac{\Delta\zeta}{\lambda_{i,j}} \quad (7)$$

$$\lambda_{i+1,j} = \frac{\lambda_{i+1,j-1} + \omega \lambda_{i,j} \psi_{i,j}}{1 + \omega \psi_{i+1,j}} \quad (8)$$

Method B:

$$\psi_{i+1,j} = \psi_{i,j} + \xi_{i,j} \frac{\Delta\zeta}{\lambda_{i,j}} \quad (9)$$

$$\lambda_{i+1,j} = \frac{-\xi_{i,j} \omega \Delta\zeta + \lambda_{i+1,j-1} + \omega \lambda_{i,j} \psi_{i,j}}{1 + \omega \psi_{i,j}} \quad (10)$$

and Method C:

$$\psi_{i+1,j} = \psi_{i,j} + \xi_{i,j} \frac{\Delta\zeta}{\lambda_{i,j}} \quad (11)$$

$$\lambda_{i+1,j} = \frac{\omega \lambda_{i,j} \psi_{i,j} - (\lambda_{i,j} - \lambda_{i,j-1})}{\omega \psi_{i+1,j}} \quad (12)$$

where, $\omega = \Delta\tau/\Delta\zeta$ represents mesh ratio of the difference schemes.

To facilitate calculation forwardly from the spinneret ($\zeta = 0$) to the take-up point ($\zeta = 1.0$), the non-dimensional spinning tension at a given time, ζ , has to be given a tentative value. Comparing the calculated taken-up velocity, $\Psi[1, \tau(j)]$, with the assumed take-up velocity, $\Psi(1, \tau)$, one reiterates revision of the non-dimensional spinning tension by employing the following Newtonian interpolation method until the error for the calculated take-up velocity becomes less than 10^{-10} of the assumed take-up velocity.

$$\xi_j^{(k+2)} = \frac{e^{(k+1)} \xi_j^{(k)} - e^{(k)} \xi_j^{(k+1)}}{e^{(k+1)} - e^{(k)}} \quad (13)$$

$$e^{(k)} = \Psi(1, \tau(j)^{(k)}) - 1.001 \psi_w \quad (14)$$

$$k = 1, 2, 3 \dots \quad (15)$$

where, ξ_j denotes the non-dimensional spinning tension at non-dimensional time $\tau = j$; $\xi_j^{(1)}$, $\xi_j^{(2)}$ are two initial tentative values; $\xi_j^{(k+2)}$ ($k = 1, 2, 3$) is the k th revised tentative value of the non-dimensional spinning tension. $e^{(k)}$ represents the difference between the calculated and assumed take-up velocities.

RESULTS AND DISCUSSION

Error Analysis of the Difference Schemes

Convergence and stability are important when a difference method is applied to solve simultaneous nonlinear partial differential equations. A definite and/or universal theory on convergence and stability, however, has not been established^[23]. It is a common practice that one investigates whether or not a difference method is convergent and stable by comparing the solution derived from the difference method with a theoretical or physical solution if it is obtainable. As long as the stability problem of a difference scheme is solved, direct numerical methods will be extremely useful in terms of the amount of information; the potential is indeed unlimited.

Figure 1 shows the simulated responses of $\lambda(1, \tau)$ to the 0.1% step increment of the take-up velocity; the draw ratio is 18.0 with $\Delta\tau = \Delta\zeta = 0.001$. The non-dimensional cross-sectional area was re-scaled so that 100% represented the cross-sectional area corresponding to the new take-up velocity after the 0.1% step increment. It is clear from the figure that the numerical solution obtained using Method B diverges from the logical value of 100%, suggesting this method has a poor stability. The error becomes smaller as a finer mesh is employed. The responses simulated using Method A and Method C are also shown in Fig. 1. The numerical solutions do converge to the logical value of 100% for both methods. Because 18.0 is below the critical draw ratio, the periodical variation in diameter rapidly decays with time.

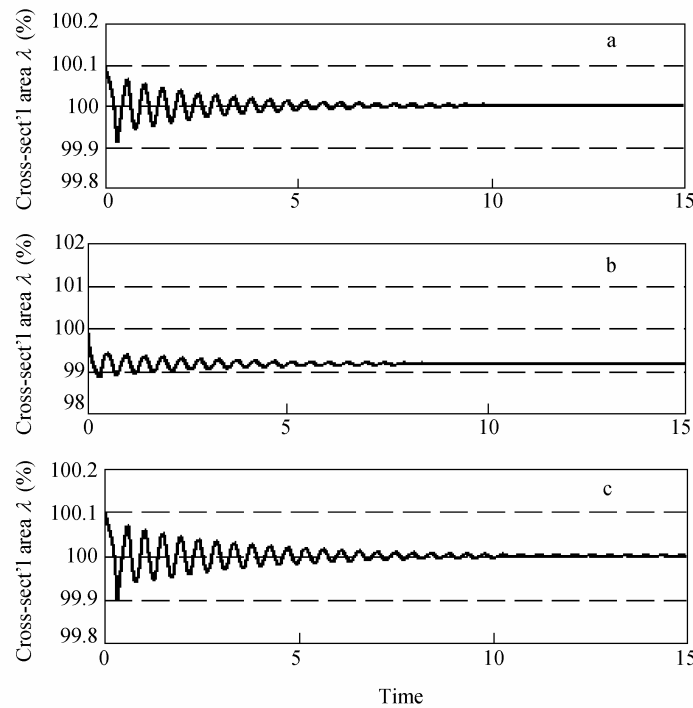


Fig. 1 Responses of cross-sectional area of taken-up filament to a 0.1% step increment in take-up velocity

Error analysis for the difference methods can be carried out by employing the Taylor series;

$$\frac{\partial \psi}{\partial \zeta} = \frac{\psi_{i+1,j} - \psi_{i,j}}{\Delta \zeta} - \frac{1}{2} \frac{\partial^2 \psi}{\partial \zeta^2} \Delta \zeta - 0(\Delta \zeta^2) \quad (16)$$

$$\frac{\partial \lambda}{\partial \zeta} = \frac{\lambda_{i+1,j} - \lambda_{i,j}}{\Delta \zeta} - \frac{1}{2} \frac{\partial^2 \lambda}{\partial \zeta^2} \Delta \zeta - 0(\Delta \zeta^2) \quad (17)$$

$$\frac{\partial \lambda}{\partial \tau} \Big|_{\text{at } i+1} = \frac{\lambda_{i+1,j} - \lambda_{i+1,j-1}}{\Delta \tau} - \frac{1}{2} \frac{\partial^2 \lambda}{\partial \tau^2} \Big|_{\text{at } i+1} \Delta \tau - 0(\Delta \tau^2) \quad (18)$$

$$\frac{\partial \lambda}{\partial \tau} \Big|_{\text{at } i} = \frac{\lambda_{i,j} - \lambda_{i,j-1}}{\Delta \tau} - \frac{1}{2} \frac{\partial^2 \lambda}{\partial \tau^2} \Big|_{\text{at } i} \Delta \tau - 0(\Delta \tau^2) \quad (19)$$

$$\frac{\partial(\lambda \psi)}{\partial \zeta} = \frac{\psi_{i+1,j} \lambda_{i+1,j} - \psi_{i,j} \lambda_{i,j}}{\Delta \zeta} - \frac{1}{2} \left[\lambda_{i,j} \frac{\partial^2 \psi}{\partial \zeta^2} + 2 \frac{\partial \lambda}{\partial \zeta} \frac{\partial \psi}{\partial \zeta} + \psi_{i,j} \frac{\partial \lambda}{\partial \zeta} \right] \Delta \zeta - 0(\Delta \zeta^2) \quad (20)$$

and spinning tension reads:

$$\xi_{i,j} = \xi_{i,j}^N + \xi_{i,j}^e \quad (21)$$

where, $\xi_{i,j}$ represents the true figure for the differential equations, $\xi_{i,j}^N$ the figure for the numerical difference equations; and $\xi_{i,j}^e$ the error. For a uniform spinning, $\xi_{i,j} = \xi_j$ as shown in Eq. (13).

Truncation errors are generated from approximation of using difference equations to replace differential equations. Substituting Eqs. (16)–(21) into Eqs. (3), (4a) and (4b), one obtains the truncation error:

$$r_{i,j}^A = \frac{1}{2(1 + \omega \psi_{i+1,j})} \left[\frac{\partial^2 \lambda}{\partial \tau^2} \Big|_{\text{at } i+1} \Delta \tau^2 + \Delta \tau \Delta \zeta \left(\lambda_{i,j} \frac{\partial^2 \psi}{\partial \zeta^2} + 2 \frac{\partial \lambda}{\partial \zeta} \frac{\partial \psi}{\partial \zeta} + \psi_{i,j} \frac{\partial^2 \lambda}{\partial \zeta^2} \right) + 0(\Delta \tau^3) + 0(\Delta \tau \Delta \zeta^2) \right] \quad (22)$$

$$r_{i,j}^B = \frac{1}{2(1 + \omega \psi_{i,j})} \left[\frac{\partial^2 \lambda}{\partial \tau^2} \Big|_{\text{at } i} \Delta \tau^2 + \psi_{i,j} \frac{\partial^2 \lambda}{\partial \zeta^2} \Delta \tau \Delta \zeta - \xi_{i,j}^e \Delta \tau + 0(\Delta \tau^3) + 0(\Delta \tau \Delta \zeta^2) \right] \quad (23)$$

$$r_{i,j}^C = \frac{1}{2\omega \psi_{i+1,j}} \left[\frac{\partial^2 \lambda}{\partial \tau^2} \Big|_{\text{at } i} \Delta \tau^2 + \Delta \tau \Delta \zeta \left(\lambda_{i,j} \frac{\partial^2 \psi}{\partial \zeta^2} + 2 \frac{\partial \lambda}{\partial \zeta} \frac{\partial \psi}{\partial \zeta} + \psi_{i,j} \frac{\partial^2 \lambda}{\partial \zeta^2} \right) + 0(\Delta \tau^3) + 0(\Delta \tau \Delta \zeta^2) \right]. \quad (24)$$

There is no need to address the pattern of error propagation for $\psi(\zeta, \tau)$ because the computed take-up velocity, $\psi(1, \tau)$, is constantly corrected in the simulation until it is within an acceptable error limit (see Eqs. (13)–(15)). Thus a significant $\xi_{i,j}^e$ would be generated in some cases as a result of compensating the truncation error to meet the error requirement for the take-up velocity, $\psi(1, \tau)$. This explains how an error occurs in simulations using Method B. On the other hand, the lower stability of Method A could be a result of using the derivatives at point $i + 1$ to replace that at point i , indicating that there is an intrinsically higher error associated with Method A than that for Method C. This can be manifested by comparing the second derivative of λ against τ in Eq. (22) with that in Eq. (24). Thus for a given mesh, Method C is better than Method A; however, Method A approaches Method C as finer and finer mesh is applied.

There is also computational rounding-off error, which can be minimised by adopting computation with long double precision. With the development of computational technology the long double data type (e.g. Borland C++) extends double precision data from 15 digit to 19 digit precision (10 bytes, there is 16 bytes long double data type as well). The computational rounding-off error is thus negligible for this study. This suggests that fine mesh is the simplest but effective way to minimise the total error.

Figure 2 shows the simulation results using Method A and Method C for a draw ratio 20.8, which is greater than the critical draw ratio 20.218^[24]. Both used the same mesh that $\Delta \tau = \Delta \zeta = 0.001$. While the amplitude of variation is seen correctly expanding with time for the curve simulated using Method C, it decays for the curve simulated using Method A. This constitutes of evidence that Method C has advantages over Method A.

Precise Critical Draw Ratio of Draw Resonance for Newtonian Fluids

The most stable method, Method C, was employed to simulate the occurrence of draw resonance in an isothermal and uniform tension melt spinning, in which ξ is a constant along the spinline, but varies with time. Displayed in

Fig. 3 is the response of the cross-sectional area of the taken-up filament to the 0.1% step increment of the take-up velocity. The cross-sectional area approaches a steady value in spite of the fact that draw ratio 20.3 is higher than the critical draw ratio 20.218. This is considered to be a result of the truncation error, indicating that the mesh used is not fine enough to simulate precise critical draw ratio. As it approaches the critical draw ratio, the simulated diameter variation lasts longer and longer. Sustained computation over a longer period is required in this case. Fortunately, increment of the computational rounding-off error resulting from a finer mesh and longer computation for the non-dimensional time is negligible due to the adoption of computation with long double precision. Given this is true, the finer the mesh, the more precise the simulation result is.

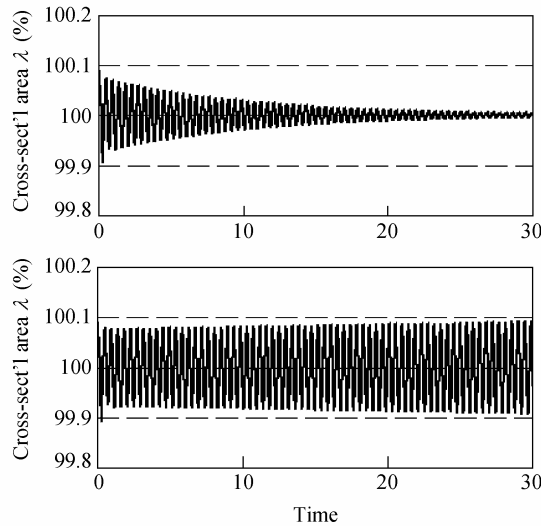


Fig. 2 Responses of the cross-sectional area of taken-up filament to a 0.1% small step increment in the take-up velocity (top: Method A; bottom: Method C)
The draw ratio before the step increment is 20.8 with $\Delta\tau = \Delta\zeta = 0.001$.

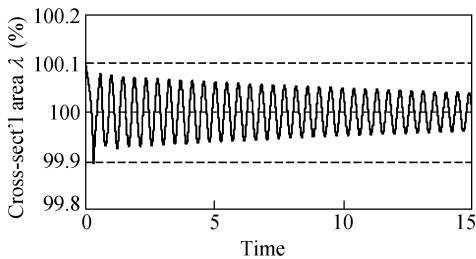


Fig. 3 Response of the cross-sectional area of taken-up filament to a 0.1% small step increment in the take-up velocity, simulated using Method C
The draw ratio before the step increment is 20.3 with $\Delta\tau = \Delta\zeta = 0.001$.

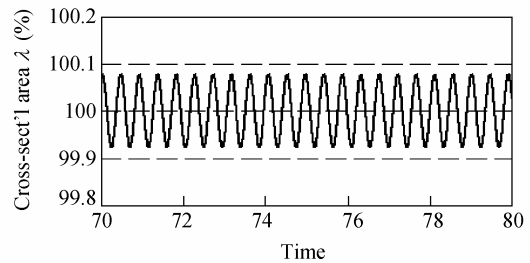
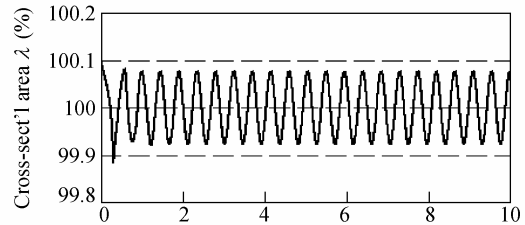


Fig. 4 Response of the cross-sectional area of taken-up filament to a 0.1% small step increment in the take-up velocity, simulated using Method C
The draw ratio before the step increment is 20.218 with $\Delta\tau = \Delta\zeta = 0.00004$. Ever lasting (almost) periodical variation in the cross-sectional area is observed.

Fine mesh of $\Delta\tau = \Delta\zeta = 0.00004$ and the acceptable error for simulated take-up velocity of less than 10^{-12} of the assumed take-up velocity were adopted to obtain the precise critical draw ratio. Displayed in Fig. 4 is the response of the take-up diameter as a function of time for a spinning with draw ratio of 20.218. The amplitude of cross-sectional area variation appears almost constant without any detectable decaying or expanding. Visual judgement based on graphical curves is no longer adequate in this case. We need to compare the change of the numerical figures for the variation over a range of non-dimensional times. For this reason, the half amplitude of the variation nearest to the select non-dimensional times was compared. Table 1 lists the results of the half amplitude for a series draw ratios close to 20.218. A clear decaying can be learnt from the table for draw ratios 20.216, 20.217 and 20.218; whilst the half amplitude expands with time for draw ratios 20.219, 20.220 and 20.221, indicating that the critical draw ratio for draw resonance in such spinning system lies in between 20.218 and 20.219. Each computation involved $(1/0.0004)^2 \times 80 = 5 \times 10^{10}$ mesh points, and took around 30 minutes for a personal computer with 800 MHz CPU frequency.

Table 1. Half amplitude (%) of cross-sectional area variation for taken-up filament with time

Draw ratio	$\tau = 5.0$	$\tau = 10.0$	$\tau = 20.0$	$\tau = 40.0$	$\tau = 60.0$	$\tau = 80.0$	Decaying or expanding
20.216	0.076713	0.076593	0.076354	0.075867	0.075383	0.074914	Decaying
20.217	0.076753	0.076673	0.076521	0.076189	0.075872	0.075549	Decaying
20.218	0.076793	0.076754	0.076674	0.076511	0.076349	0.076190	Decaying
20.219	0.076834	0.076834	0.076834	0.076835	0.076836	0.076837	Expanding
20.220	0.076874	0.076914	0.076995	0.077160	0.077326	0.077488	Expanding
20.221	0.076914	0.076995	0.077156	0.077480	0.077819	0.078146	Expanding

The critical draw ratio was only identified to be between 7.4 and 20.1 by using a direct difference method to solve the governing equations in such a spinning in the literature^[15, 18]. A previous study^[17] demonstrated the critical draw ratio is between 20 and 21. This present simulation has verified, using direct difference method, the critical draw ratio is 20.218. Given the advantage of full information for a direct difference method capable to provide, it is expected that direct difference methods will receive more and more attention.

CONCLUSION

Computation with 19 digit long double precision has significantly simplified the stability problem of difference equations for melt spinning. For unsteady simulation of melt spinning, numerical stability can always be improved by simply adopting a finer mesh to minimise the truncation error without increasing the computational rounding-off error. In addition, error analysis has found that a difference scheme with its derivatives closer to the mesh point ij has higher stability. For Newtonian fluids in an isothermal and uniform tension spinning, the critical draw ratio is found to lie in between 20.218 and 20.219, a perfectly consistent figure with 20.218. This has paved the way to computation of full information for unsteady melt spinning processes using the difference method.

REFERENCES

- 1 Cao, J., *J. Appl. Polym. Sci.*, 1991 42: 143
- 2 Cao, J., *J. Appl. Polym. Sci.*, 1992, 45: 2169
- 3 Han, C.D. and Kim, Y.W., *J. Appl. Polym. Sci.*, 1976, 20: 1583
- 4 Kase, S., *J. Appl. Polym. Sci.*, 1974, 18: 3279
- 5 Kase, S. and Matsuo, T., *J. Appl. Polym. Sci.*, 1965, A3: 2541
- 6 Kase, S. and Matsuo, T., *J. Appl. Polym. Sci.*, 1967, 11: 251
- 7 Matsumoto, T. and Bogue, D.C., *Polym. Eng. Sci.*, 1978, 18: 564
- 8 Tsou, J.D. and Bogue, D. C., *J. Non-Newtonian Fluid Mech.*, 1985, 17: 331

- 9 White, J.L., *Polym. Eng. Rev.*, 1981, 11: 297
- 10 Petrie, C.J. and Denn, M.M., *AIChE J.*, 1976, 22: 209
- 11 Fisher, R.T. and Denn, M.M., *AIChE J.*, 1976 22: 236
- 12 Pearson, J.R.A. and Matovich, M.A., *Ind. Eng. Chem.: Fundamentals*, 1969, 8: 605
- 13 Pearson, J.R.A. and Shah, Y.T., *Trans. Soc. Rheo.*, 1972, 16(3): 519
- 14 Pearson, J.R.A. and Shah, Y.T., *Ind. Eng. Chem.: Fundamentals*, 1974, 13: 134
- 15 Toriumi, K. and Konda, A., *Sen-i Gakkaishi*, 1984, 40: 193
- 16 Van der Hout, R., *Eur. J. Appl. Math.*, 2000, 11(2): 129
- 17 Cao, J., *J. Appl. Polym. Sci.*, 1993, 49: 1759
- 18 Ishihara, H. and Kase, S., *J. Appl. Polym. Sci.*, 1975, 19: 557
- 19 Ishihara, H. and Kase, S., *J. Appl. Polym. Sci.*, 1976, 20: 169
- 20 Kim, B.M., Hyun, J.C., Oh, J.S. and Lee, S.J., *AIChE J.*, 1996, 42(11): 3164
- 21 Jung, H.W., Song, H.S. and Hyun, J.C., *AIChE J.*, 2000, 46 (10): 2106
- 22 Lee, J.S., Jung, H.W., Kim, S. H. and Hyun, J.C., *J. Non-Newtonian Fluid Mech.*, 2001, 99(2-3): 159
- 23 Lax, P.D., *Comm. Pure and Appl. Math.*, 1960, 13: 217
- 24 Kase, S. and Denn, M.M., "Proc. 1978 Joint Automatic Control Conf. II-71", Pittsburgh, USA, 1978

Copyright of Chinese Journal of Polymer Science is the property of World Scientific Publishing Company and its content may not be copied or emailed to multiple sites or posted to a listserv without the copyright holder's express written permission. However, users may print, download, or email articles for individual use.